

Enzyme specific activity in functionalized nanoporous supports

Chenghong Lei, Thereza A Soares, Yongsoon Shin, Jun Liu and Eric J Ackerman

Pacific Northwest National Laboratory, PO Box 999, Richland, WA 99352, USA

E-mail: Eric.Ackerman@pnl.gov

Received 19 October 2007, in final form 17 January 2008

Published 20 February 2008

Online at stacks.iop.org/Nano/19/125102

Abstract

Here we reveal that enzyme specific activity can be increased substantially by changing the protein loading density (P_{LD}) in functionalized nanoporous supports so that the enzyme immobilization efficiency (I_e , defined as the ratio of the specific activity of the immobilized enzyme to the specific activity of the free enzyme in solution) can be much higher than 100%. A net negatively charged glucose oxidase (GOX) and a net positively charged organophosphorus hydrolase (OPH) were entrapped spontaneously in NH_2 - and HOOC-functionalized mesoporous silica (300 Å, FMS) respectively. The specific activity of GOX entrapped in FMS increased with decreasing P_{LD} . With decreasing P_{LD} , I_e of GOX in FMS increased from <35% to >150%. Unlike GOX, OPH in HOOC-FMS showed increased specific activity with increasing P_{LD} . With increasing P_{LD} , the corresponding I_e of OPH in FMS increased from 100% to >200%. A protein structure-based analysis of the protein surface charges directing the electrostatic interaction-based orientation of the protein molecules in FMS demonstrates that substrate access to GOX molecules in FMS is limited at high P_{LD} , consequently lowering the GOX specific activity. In contrast, substrate access to OPH molecules in FMS remains open at high P_{LD} and may promote a more favorable confinement environment that enhances the OPH activity.

(Some figures in this article are in colour only in the electronic version)

 Supplementary data are available from stacks.iop.org/Nano/19/125102

1. Introduction

The specific activity of immobilized enzymes using conventional immobilization supports such as sol-gel silica is usually lower than, or much lower than, that of the free enzymes in solution because of small pore sizes, non-open pore structures and harsh immobilization conditions [1–6]. With rigid and open large pore structures and controllable pore sizes, mesoporous silica can facilitate mass transport of the enzyme substrate and product, and allow the enzyme to be spontaneously entrapped inside the mesopores under neutral mild conditions. Recently, both unfunctionalized and functionalized mesoporous silica (UMS and FMS) have been tested as new enzyme immobilization strategies [7–15]. Han and Deere *et al* reported that the pH and ionic strength of buffer solutions have a large effect on the protein amounts immobilized because the electrostatic inter-

actions dominate between the enzymes and the mesoporous surfaces [9, 10].

The positive charges of a protein are attributable to a surplus of surface amino groups in lysines, arginines and/or histidines, while the negative charges result from a surplus of surface carboxylic groups in glutamates and/or aspartates. Because amino groups and carboxyl groups form a naturally electrostatic couple in aqueous solution, one enzyme immobilization strategy can use the high affinity of NH_2 - and HOOC-FMS to allow negatively charged and positively charged enzymes respectively to be spontaneously entrapped. Functional HOOC- and NH_2 - groups would offer potential electrostatic, H-bond and hydrophilic interactions with the charged amino acid residues of protein molecules. Our previous work reported a dramatic increase of enzyme loading in both enzyme activity and protein amount when using NH_2 -FMS and HOOC-FMS in comparison with UMS

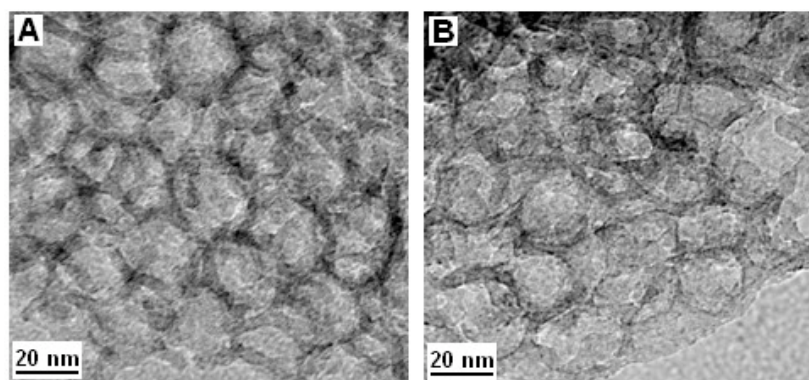


Figure 1. TEM images of 300 Å UMS (A), and the corresponding 2% HOOC-FMS (B).

and normal porous silica [7, 8]. The results showed that the electrostatic interaction, functionalization and mesoporous nanostructures are paramount for enzyme entrapment [7, 8]. Our preliminary data indicated that enzyme specific activity could be significantly affected by the protein loading density in FMS [8].

By conventional immobilization methods, the activities of the immobilized enzymes are obtained when the proteins are loaded under saturating conditions [1–6]. Here we report that the enzyme specific activities correlate with the protein loading densities in FMS and how these correlations are governed by the enzyme orientations in FMS.

2. Experimental details

2.1. Preparation of enzyme–FMS composites

Mesoporous silica (SBA-15) with $533 \text{ m}^2 \text{ g}^{-1}$ surface area and 300 Å pore size, and the corresponding NH_2 -FMS and HOOC-FMS were from the same batch prepared for the previous work [7, 8, 16, 17]. In a typical preparation of mesoporous silica with 300 Å pores, 12.0 g of Pluronic P-123 (MW = 5800) was dissolved in 2 M HCl solution (360 ml) at 40 °C. Then 18.0 g of mesitylene and 25.5 g of tetraethylorthosilicate (TEOS) were added to the milky solution and stirred for 18 h at the same temperature. The mixture was transferred into a Teflon-lined autoclave and heated up to 100 °C for 24 h without stirring. The white precipitate was collected by filtration, dried in air, and then calcined at 550 °C for 6 h.

A controlled hydration and condensation reaction was used to introduce functional groups into UMS [16]. The amount of trimethoxy silanes needed was calculated based on the fraction of the surface area to be occupied by silane molecules; for example, 2% (or 20%) coverage of HOOC-FMS or NH_2 -FMS means 2% (or 20%) of the total available surface area of the mesoporous silica would be silanized with the trimethoxy silane with the functional group HOOC– or NH_2 –. For UMS (300 Å pore size), the coverage of 2% corresponds to $\sim 0.09 \text{ mmol silane/g}$ assuming $5 \times 10^{18} \text{ molecules m}^{-2}$ in a fully dense monolayer coverage, as indicated by previous solid-state NMR studies [16]. In a typical procedure of 2% HOOC-FMS synthesis (300 Å pores), 1.0 g of mesoporous silica was first suspended in toluene (60 ml) and pretreated

with water (0.32 ml) in a three-necked, 250 ml round-bottomed flask, which was fitted with a stopper and reflux condenser. This suspension was stirred vigorously for 2 h to distribute the water throughout the mesoporous matrix, during which time it became a thick, homogeneous slurry. At this point, 15.5 mg of tris-(methoxy)cianoethylsilane (TMCES, MW = 175.26) was added, and the mixture was refluxed for 6 h. The mixture was allowed to cool to room temperature and the product was collected by vacuum filtration. The treated mesoporous silica was washed with ethyl alcohol repeatedly and dried under vacuum. To hydrolyze cyano groups (CN– would be hydrolyzed into HOOC– as the functional group), 10 ml of 50% of H_2SO_4 solution was added to the mixture, which was then refluxed for 3 h. The product was filtered off and washed with water extensively. Other samples were synthesized by the same procedure except different amounts of organosilanes were added based on their surface areas, and no hydrolysis step was needed when functionalizing with tris-(methoxy)aminopropylsilane (TMAPS, NH_2 – as the functional group). Figure 1 shows the transmission electron microscopy (TEM) images of UMS and 2% HOOC-FMS. As expected, there is no significant difference between the two TEM images, so overall mesoporous pore structures were maintained after functionalization. Unlike 30 and 100 Å mesoporous silica, the 300 Å mesoporous silica has a large degree of disordering [17], but the pore sizes are more or less uniform [18]. Typical Brunauer–Emmett–Teller (BET) and x-ray diffraction (XRD) data of UMS and 20% HOOC-FMS are included in the supporting information (available at stacks.iop.org/Nano/19/125102). Because the molecular chains in the large pore channels have multilayer structures [18], the pore sizes of 20% HOOC-FMS were reduced to 170 Å due to the functionalization.

An aliquot of 2.0–8.0 mg of FMS or other silica support was added in a 1.8 ml tube for incubation at 25 °C with 200–1200 μl of the enzyme stock. The incubation tubes were shaken at 1400 min^{-1} on an Eppendorf Thermomixer 5436 for 2–3 h. The enzyme stock in the absence of FMS was also shaken under the same conditions for comparison. In this work, the working buffers were pH 7.5, 20 mM HEPES for OPH and pH 7.0, 20 mM sodium phosphate (in the presence or absence of 0.15 M NaCl) for GOX.

Based on the preliminary experiments, 0.1–0.2 mg protein was used for incubation per mg of silica support so that the enzyme was in excess. Then the enzyme–FMS composite was repeatedly separated by centrifugation and washed in the working buffer at room temperature ($21 \pm 1^\circ\text{C}$) until both the protein and enzyme activity were undetectable in the supernatant. Finally, the washed deposit was resuspended in 100–300 μl of the working buffer per mg of original FMS for further protein and activity measurement.

For the studies on the correlation of the enzyme specific activity with the protein loading density in FMS, limiting amounts of enzyme were incubated in aliquots of FMS to produce lower protein loading densities. For these observations, the total protein amount was known for each incubation, and the total enzyme activity was measured comprising the enzyme–FMS composite and any unbound enzyme in the incubation solution. The enzyme activity and the protein amount remaining in the incubation solution were measured separately. After subtracting the enzyme activity and the protein amount remaining in the incubation solution from the total enzyme activity and the total protein amount, the enzyme activity and the protein amount immobilized in FMS were obtained.

2.2. Measurement and characterization

The mass amount of proteins was measured using a Pierce BCA assay kit (Pierce, Product 23227). To avoid any scattering during spectrophotometric measurement of protein amounts, the silica particles were removed by centrifugation after the enzyme–FMS composite was incubated with the working reagent.

OPH was cloned, expressed, purified, dialyzed, and stored at -80°C [7]. It was thawed at 4°C and diluted in pH 7.0–7.5, 0.1 M HEPES before use. OPH activity was measured in 1 mM of paraoxon in pH 9.0, 0.15 M CHES buffer at 25°C , in which one OPH unit is the active amount allowing 1.0 μmol paraoxon to be hydrolyzed per minute. OPH stock solution and OPH–FMS suspension were diluted 10–50 times by pH 7.5, 20 mM HEPES for activity measurements. Multiple batches of OPH stock solutions, which had different initial specific activities in the range of 700–5000 units mg^{-1} , were used for this work. GOX activity was measured using the standard protocol from Sigma (revised 08/30/1996). About 10 mg of GOX (Sigma G-7016) was dissolved in 5 ml of pH 7.0, 20 mM sodium phosphate in the presence (absence) of 0.15 M NaCl as the GOX stock used for this work, which had an initial specific activity of 280.0–310.0 units mg^{-1} .

A Hewlett Packard 8452A diode array spectrophotometer was used to record all UV–visible spectra for activity measurement. High resolution TEM was carried out on a Jeol JEM 2010 microscope. The operating voltage on the microscope was 200 kV.

2.3. Electrostatic charge calculations

The net charges of surface regions for the crystallographic structures of OPH (Protein Data Bank ID: 1HZY) and GOX (Protein Data Bank ID: 1GAL) were calculated using an

online resource at EMBL (WWW Gateway to Isoelectric Point Service: <http://www.embl-heidelberg.de/cgi/pi-wrapper.pl>).

Full distributions of the electrostatic charges of the two proteins were calculated by solving the linearized Poisson–Boltzmann equation with the Adaptive Poisson–Boltzmann Solver package [19]. This model has been extensively applied to biological molecules, and the details of its implementation were described earlier [20–22]. The differential Poisson equation describes the electrostatic charge $\Phi(r)$ in a medium with a dielectric scalar field $\varepsilon(r)$ and with a charge density $\rho(r)$:

$$\nabla \cdot \varepsilon(r) \nabla \Phi(r) = -4\pi \rho(r). \quad (1)$$

In a solvated molecular system, the charge density is divided into the fixed interior charge distribution of the molecule, $\rho_{\text{int}}(r)$, and a mobile exterior charge density of the solvent and ions. The exterior is modeled as a dielectric continuum with the mobile ion density approximated by a Boltzmann distribution at temperature T . Therefore, equation (1) takes the form of the nonlinear Poisson–Boltzmann equation:

$$\nabla \cdot \varepsilon(r) \nabla \Phi(r) = -4\pi \rho_{\text{int}}(r) + \lambda(r) \kappa^2 \sinh[\Phi(r)/kT], \quad (2)$$

where $\varepsilon(r)$ is the dielectric constant of the solute or the solvent, k is the Boltzmann constant, and λ equals 1 for ion-accessible regions and 0 elsewhere. κ^2 is the modified Debye–Hückel parameter, defined as

$$\kappa^2 = \frac{8\pi N_A I}{1000kT}. \quad (3)$$

The nonlinear Poisson–Boltzmann equation can then be simplified into the linear Poisson–Boltzmann equation:

$$\nabla \cdot \varepsilon(r) \nabla \Phi(r) = -4\pi \rho_{\text{int}}(r) + \lambda(r) \kappa^2 \Phi(r). \quad (4)$$

For the electrostatic calculations, hydrogens were added to the crystallographic coordinates by using the PDB2PQR software [23]. Partial charges and atomic radii were taken from the AMBER force field. The solute and solvent were assigned a dielectric constant of 2 and 78.5, respectively. The ionic strength of monovalent ions was set to 0.150 M with an ion exclusion radius of 2 Å and a temperature of 298 K. The finite-difference Poisson–Boltzmann calculations employed a $129 \times 129 \times 129 \text{ \AA}^3$ grid with a 0.5 Å spacing between grid points.

3. Results and discussion

3.1. OPH and GOX spontaneously entrapped in FMS via electrostatic interactions

Hexagonally ordered mesoporous silica (SBA-15) with pore sizes of 300 Å and the corresponding FMS were from the same batch prepared in the previous work [7, 8]. FMS was incubated in the enzyme stock solution (see section 2), thereby avoiding harsh immobilization conditions that destroy enzymatic activity. We define the protein amount (mg) of an enzyme immobilized with 1 g of an FMS support as the protein

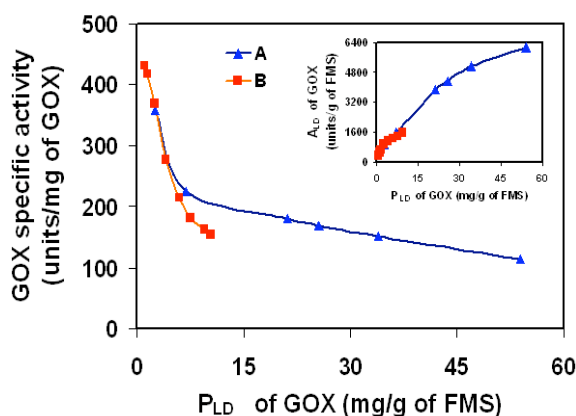


Figure 2. Increase of GOX specific activity with decreasing P_{LD} of GOX in 20% NH_2 -FMS. (A) GOX-FMS in pH 7.0, 20 mM sodium phosphate; the specific activity of GOX stock for incubation was 295.2 units mg^{-1} ; (B) GOX-FMS in pH 7.0, 20 mM sodium phosphate containing 0.15 M NaCl; the specific activity of GOX stock for incubation was 281.5 units mg^{-1} .

loading density (P_{LD}), and the corresponding activity (units) as the activity loading density (A_{LD}). The immobilization efficiency (I_e) is defined as the ratio of the specific activity of the immobilized enzyme (A_{LD}/P_{LD}) to the specific activity of the free enzyme in stock solution. Based on the preliminary experiments, 0.1–0.2 mg protein was used per mg of FMS so that the enzyme was in excess for incubation. Alternatively, lower amounts of enzyme were incubated with aliquots of FMS so that different P_{LD} could be obtained. Protein amount and enzyme activity measurements are described in section 2.

When the pH is greater than the pI of GOX (4.0), the negatively charged GOX were spontaneously entrapped in NH_2 -FMS [8]. In pH 7.0, 20 mM sodium phosphate buffer, when GOX was in excess for incubation, P_{LD} of GOX entrapped in 300 Å 20% NH_2 -FMS was 79.8 mg g^{-1} of FMS, with a specific activity of 102.9 units mg^{-1} , resulting in an I_e of 34.8% (the specific activity of the initial GOX stock solution was 295.2 units mg^{-1}). With the oppositely charged 20% HOOC-FMS, P_{LD} of GOX entrapped was only 7.4 mg g^{-1} of FMS. In pH 7.0, 20 mM sodium phosphate buffer containing 0.15 M NaCl, P_{LD} of GOX entrapped in 20% NH_2 -FMS was reduced dramatically to 14.6 mg g^{-1} of FMS. These results demonstrated that the electrostatic interaction dominated between FMS and GOX.

In contrast to negatively charged GOX, when the pH was below the pI of OPH (8.3), the positively charged OPH (with a surplus of NH_2 -residues) interacted favorably with HOOC-FMS [7]. In pH 7.5, 20 mM HEPES, P_{LD} of OPH entrapped in 300 Å 2% and 20% HOOC-FMS was 46.7 and 32.2 mg g^{-1} of FMS, with the specific activities of 4182 and 4108 units mg^{-1} , resulting in I_e of 216.9% and 213.1% respectively (the specific activity of the initial OPH stock solution was 1928 units mg^{-1}). OPH was almost completely repelled by 20% NH_2 -FMS as expected. The electrostatic interactions were further confirmed by increasing the buffer concentration to 100 mM HEPES; P_{LD} of OPH entrapped in 2% HOOC-FMS was reduced to

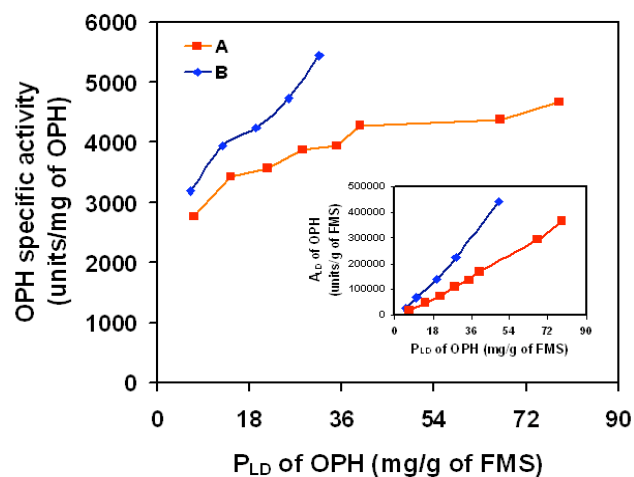


Figure 3. Increase of OPH specific activity with increasing P_{LD} of OPH in 2% HOOC-FMS. (A) The specific activity of the OPH stock solution prior to the entrapping was 2602.5 units mg^{-1} ; (B) the specific activity of the OPH stock solution prior to the entrapping was 4658.8 units mg^{-1} .

30.8 mg g^{-1} of FMS. The binding affinities of OPH and GOX in FMS were correlated with their respective pI values, suggesting a prominent role of electrostatic interactions in the spontaneous entrapping process. In comparison with FMS, UMS and normal porous silica (whether functionalized or not) exhibited substantially lower P_{LD} and A_{LD} than FMS [7, 8].

3.2. Effects of protein loading density of GOX in FMS on enzyme specific activity

The above-mentioned results indicate that I_e for GOX in 20% NH_2 -FMS, and OPH in 2% or 20% HOOC-FMS were significantly different—~35% versus ~200% respectively. Interestingly, the specific activity of GOX in FMS could increase with a lowered P_{LD} when less GOX was incubated with FMS. When FMS exceeded lower amounts of GOX, a series of low P_{LD} was obtained. The less GOX used for incubation, the lower the P_{LD} , and the higher the specific activity. When P_{LD} was 2.6 mg g^{-1} of FMS in pH 7.0, 20 mM sodium phosphate (figure 2(A)), the GOX specific activity in FMS could reach as high as 357.4 units mg^{-1} , resulting in an I_e of 121%. Because of the higher ionic strength, a lower range of P_{LD} of GOX in FMS was obtained in the same buffer in the presence of 0.15 M NaCl (figure 2(B)). When P_{LD} was 1.2 mg g^{-1} of FMS (figure 2(B)), the GOX specific activity in FMS could reach as high as 431.2 units mg^{-1} , resulting in an I_e of 153%. This was a remarkable change compared with the much lower I_e (<35%) when FMS was incubated in excess of GOX. Figure 2 shows that, when P_{LD} of GOX was below 4.0 mg g^{-1} of FMS, I_e was $\geq 100\%$. These results demonstrated that the specific activity of GOX could be much improved by limiting the amount of enzyme in FMS, indicating that FMS as a confined space could enhance GOX activity only when P_{LD} was essentially low. The inset of figure 2 shows the increasing A_{LD} with the increasing P_{LD} , although with decreasing specific activity. When FMS was incubated

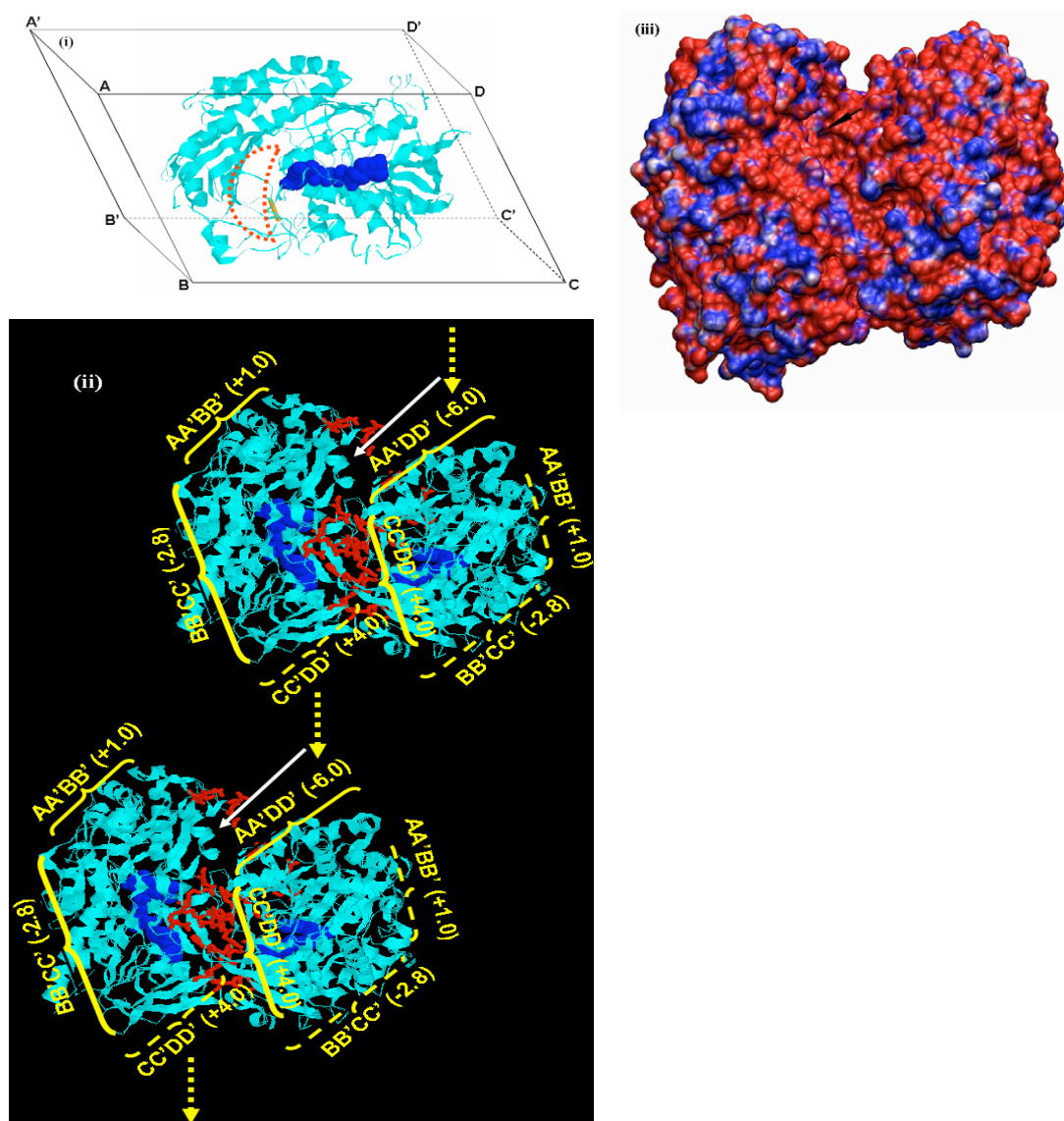


Figure 4. (i) Crystal structure of the GOX monomer in a suppositional inclined cuboid (ABCD–A'B'C'D'), where the region containing both the entrance for substrate access (the area outlined in red dashed line) and the monomer–interface surface faces outside the plane of the paper (side ABCD). Flavin adenine dinucleotide (FAD) in the active site is displayed in blue van der Waals radii. The majority of the protein is displayed by cyan ‘ribbons’ [29]. (ii) GOX dimers in FMS. The two monomers of the dimer are interfaced with 120 contact points around 11 residues (in red sticks) that form either salt linkages or hydrogen bonds between the surface region of one monomer facing side ABCD and the same region of the other monomer [29]. Access to FAD is provided by a large deep pocket which is shaped like a funnel (white arrow) [29]. The local region containing the surface facing side AA'DD' of the left monomer of the GOX dimer is depicted as attaching to the FMS wall (dark background), leaving the same region of the right monomer exposed. Other related regions of two monomers are marked with net charge numbers. Potential aggregation of the GOX dimers at higher P_{LD} is depicted by yellow dotted arrows. (iii) Colored electrostatic charge distribution on the molecular surface of GOX corresponding to that displayed in (ii). The blue color represents strong positive charge whereas the red color represents strong negative charge [19–23]. The scale of the surface charge is given in $k_B T$ and in the range between -5 and $5 k_B T$.

with excess GOX, some GOX molecules might aggregate in the FMS. The aggregated molecules would likely be denatured and could also exert unfavorable mass transport effects by restricting substrate access to the active site that could lower the enzyme specific activity. While multiple explanations for the decreasing specific activity such as aggregation, denaturation, or the substrate-channeling effects of the counter ions on protein surfaces are possible, our previous results demonstrated that FMS actually prevents denaturing and even promotes renaturing of the entrapped proteins [8, 24]. An

analysis of regional net charges for GOX suggests that the specific activity of GOX in FMS is related to its orientation in FMS based on electrostatic interactions as described below.

3.3. Effects of protein loading density of OPH in FMS on enzyme specific activity

We observed that I_e of OPH in FMS could reach $>200\%$, indicating that some misfolded/unfolded enzyme in solution might be refolded and accordingly renatured in HOOC-FMS.

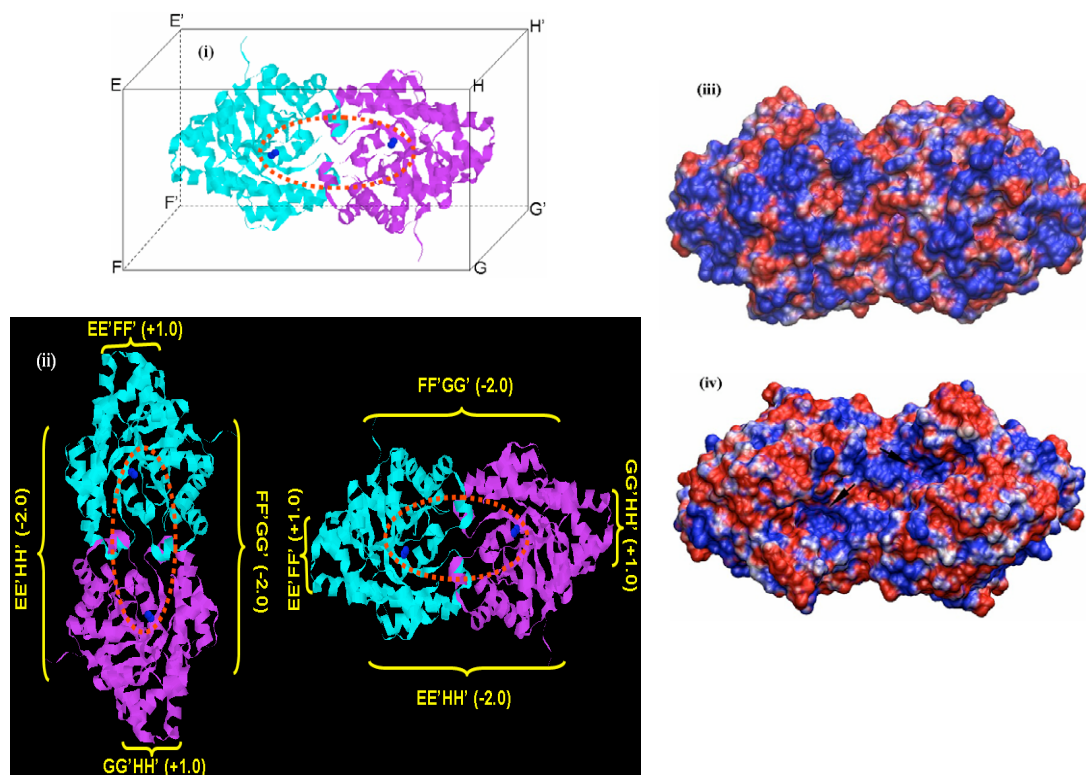


Figure 5. (i) The crystal structure of the OPH dimer in a suppositional cuboid ($EFGH-E'F'G'H'$), where the region containing the entrance for substrate access (outlined by the red dashed line) and the interfacing sites of the two monomers faces outside the plane of the paper (side $EFGH$). Metal ions (Zn^{2+} , or Co^{2+}) in the active site are displayed in blue-colored van der Waals radii. The majority of the two identical monomers are displayed by cyan and magenta 'ribbons' respectively. (ii) The symmetrical structure with two small positively charged regions and two negatively charged regions allows the largest positively charged region ($+8.0$), the opposite region to the substrate access entrance, to attach to the FMS wall (dark background), leaving the entrance completely open; (iii) the back view (facing side $E'F'G'H'$) and (iv) the front view (facing side $EFGH$) of colored electrostatic charge distribution on the molecular surface of OPH corresponding to that displayed in (ii), where the blue color represents strong positive charge and the red color represents strong negative charge [19–23]. The scale of the surface charge is given in $k_B T$ and is in the range between -5 and $5 k_B T$.

When we added different amounts of OPH from the same batch of OPH solution for incubation in several aliquots of FMS, a series of P_{LD} was obtained. We found that OPH in HOOC-FMS showed increased specific activity with increasing P_{LD} . For one OPH stock solution with an initial specific activity of $2602.5 \text{ units mg}^{-1}$ prior to entrapping, when P_{LD} of OPH in FMS increased from 7.2 to 78.4 mg g^{-1} of FMS, I_e could increase from 106% to 179% (figure 3(A)). For another OPH stock solution with an initial specific activity of $4658.8 \text{ units mg}^{-1}$, when P_{LD} increased from 5.2 to 48.2 mg g^{-1} of FMS, I_e could increase from 114% to 194% (figure 3(B)). The inset of figure 3 shows the increasing A_{LD} with the increasing P_{LD} as expected. The results demonstrated that the aggregation did not occur with OPH as it may have done with GOX; instead OPH entrapped in FMS at a higher P_{LD} might offer a more favored 'molecular crowding' environment [25–28], where neighboring OPH molecules could enhance their activities. The I_e varied from sample to sample, indicating that the specific activity of OPH entrapped in FMS is related to the initial specific activity and the initial ratio of the inactive to active protein of the free enzyme prior to entrapping.

3.4. Regional net charges of GOX and its orientation in FMS

Why did a higher P_{LD} of GOX in FMS yield a lower specific activity, while a higher P_{LD} of OPH result in a higher specific activity? To address this question, although GOX is net negatively charged at pH 7.0 and OPH is net positively charged at pH 7.5, we performed a preliminary analysis of the regional net charges for GOX and OPH to determine their orientations in FMS based on electrostatic interactions.

GOX (Protein Data Bank ID: 1GAL) consists of two identical monomers [29]. The local regions containing the entrance for substrate access of each monomer of the dimeric GOX molecule are asymmetrically interfaced; thereby, access to the enzyme active site is provided by a large deep pocket which is shaped like a funnel (figure 4) [29]. To calculate the regional net charges of the GOX dimer, the crystal structure of the GOX monomer was assumed in an inclined cuboid $ABCD-A'B'C'D'$ considering the monomer's inclined shape (figure 4(i)) and the dimer's special structure where the local region facing side $ABCD$ contains both the entrance for substrate access and the monomer interfacing surface (figure 4(ii)). The charged amino acid residues and the calculated net charges of surface regions of the GOX monomer are summarized in table 1. Figure 4(iii) shows a colored

Table 1. The net charges of surface regions of the GOX monomer at pH 7.0. (Calculated using an online resource at EMBL WWW Gateway to Isoelectric Point Service: <http://www.embl-heidelberg.de/cgi/pi-wrapper.pl>.)

Surface region facing sides	Charged amino acid residues	Regional net charges
AA'DD'	ASP497, ASP499, ASP360, GLU505, GLU367, GLU458, GLU379, GLU378, GLU363, LYS364, LYS372, ARG383	-6.0
A'B'C'D'	ASP134, ASP120, ASP573, ASP578, ASP401, ASP208, ASP203, GLU123, GLU129, GLU577, LYS570, LYS201, LYS202, LYS116, ARG147, ARG37, ARG145, ARG400, HIS115, HIS210, HIS158, HIS406, HIS165	-1.5
BB'CC'	ASP181, ASP180, ASP177, ASP57, ASP222, GLU221, GLU231, GLU40, GLU5, LYS152, HIS220, HIS172, ARG147, ARG145, ARG230, ARG239	-2.8
AA'BB'	LYS152, LYS201, LYS187, ARG337, ARG472, ASP181, ASP195, GLU194, GLU487	+1.0
CC'DD'	LYS306, LYS441, LYS252, LYS273, LYS13, LYS282, ARG263, HIS277, ASP315, GLU310, GLU268	+4.0

Table 2. The net charges of surface regions of OPH at pH 7.5. (Calculated using an online resource at EMBL WWW Gateway to Isoelectric Point Service: <http://www.embl-heidelberg.de/cgi/pi-wrapper.pl>.)

Surface region facing sides ^a	Charged amino acid residues	Regional net charges
EE'HH'	ASP35, ASP315, ASP318, ASP323, ASP264, GLU217, GLU219, GLU144, GLU145, GLU71, GLU81, GLU263, LYS77, ARG363, ARG36, ARG225, ARG246, ARG164, ARG85, ARG89, ARG319, ARG331	-2.0
E'F'G'H'	ASP160A, ASP121A, ASP109A, ASP35A, GLU159A, GLU48A, GLU81A, LYS77A, ARG152A, ARG67A, ARG164A, ARG76A, ARG36A, ARG96A, ARG91A, ARG88A, ARG89A, ARG85A, ASP160B, ASP121B, ASP109B, ASP35B, GLU159B, GLU48B, GLU81B, LYS77B, ARG152B, ARG67B, ARG164B, ARG76B, ARG36B, ARG96B, ARG91B, ARG88B, ARG89B, ARG85B	+8.0
FF'GG'	ASP35, ASP315, ASP318, ASP323, ASP264, GLU217, GLU219, GLU144, GLU145, GLU71, GLU81, GLU263, LYS77, ARG363, ARG36, ARG225, ARG246, ARG164, ARG85, ARG89, ARG319, ARG331	-2.0
EE'FF'	LYS294A, LYS285A, LYS339A, ARG337A, ASP289A, GLU344A, GLU338A	+1.0
GG'HH'	LYS294B, LYS285B, LYS339B, ARG337B, ASP289B, GLU344B, GLU338B	+1.0

^a Because of the symmetrical interfacing of two identical monomers, the regions facing EE'HH' and FF'GG' have the same sequence of charged surface amino residues; so do the regions facing EE'FF' and GG'HH'.

electrostatic charge distribution on the molecular surface of GOX corresponding to that displayed in figure 4(ii). Because electrostatic interactions exert a prominent role between GOX and NH₂-FMS, the local region of GOX containing the surface facing side AA'DD' with the largest number of negative charges (−6.0) (table 1) should favor attachment to the positively charged wall of NH₂-FMS (dark background, figure 4(ii)), leaving the funnel for substrate access of the dimer opening horizontally along the FMS wall. This orientation of the GOX dimers in FMS would result in the substrate access funnel of one dimer being readily susceptible to being blocked by another dimer, or one dimer presenting as a steric barrier for the substrate access entrance of another dimer at higher P_{LD} (figure 4(ii)), thereby forming aggregated dimers that would significantly lower the enzymatic activity. Accordingly, at higher P_{LD} of GOX in FMS, the more GOX molecules might aggregate, and thereby yield lower specific activity. This is in agreement with the previous report that the monomers of GOX are linked by non-covalent bonds, and that the dimer and trimer possess enzymatic activity, but the tetramer does not [30].

3.5. Regional net charges of OPH and its orientation in FMS

OPH (Protein Data Bank ID: 1HZY) also consists of two identical monomers [31]. Unlike GOX, the two monomers of OPH are symmetrically linked to form an open entrance for substrate access [31]. The regional net charges were calculated assuming the crystal structure of the OPH dimer in a cuboid EFGH–E'F'G'H' (figure 5(i)). The charged amino acid residues and the calculated net charges of surface regions of OPH are summarized in table 2. Figures 5(iii) and (iv) show the back view (facing side E'F'G'H') and the front view (facing side EFGH) of colored electrostatic charge distribution on the molecular surface of OPH corresponding to that displayed in figure 5(ii), respectively. Interestingly, the local region of OPH containing the surface facing side E'F'G'H' with the largest number of positive charges (+8.0) (table 2) is in the opposite side to the substrate entrance (facing side EFGH). Unlike GOX, when this positively charged region of OPH attaches to the negatively charged wall of HOOC-FMS (dark background, figure 5(ii)), the substrate access entrance of OPH opens perpendicularly against the FMS wall, leaving a completely open entrance for substrate. Therefore, there was no unfavorable aggregation of OPH in FMS as occurred with GOX. Instead, a higher P_{LD} of OPH in FMS presented a more favorable molecularly crowded confinement space that could enhance the enzymatic activity [25–28].

In conclusion, based on the results from GOX and OPH entrapment in NH₂-FMS and HOOC-FMS respectively, the enzyme specific activity in FMS and the resulting immobilization efficiency significantly rely on the protein loading density. How the protein loading density affects the enzyme specific activity can be correlated with the orientations of proteins in FMS. Optimizing structural characteristics of FMS and proteins will improve the specific activities of the enzymes immobilized in FMS.

Acknowledgments

We gratefully acknowledge funding of this work by the US Department of Energy Office of Biological and Environmental Research and Basic Energy Sciences under Contract DE-AC06-RLO1830.

References

- [1] Bhatia R B and Brinker C J 2000 Aqueous sol–gel process for protein encapsulation *Chem. Mater.* **12** 2434–41
- [2] Braun S, Rappoport S, Zusman R, Avnir D and Ottolenghi M 1990 Biochemically active sol–gel glasses: the trapping of enzymes *Mater. Lett.* **10** 1–5
- [3] Glad M, Norrlof O, Sellergren B, Siegbahn N and Mosbach K 1985 Use of silane monomers for molecular imprinting and enzyme entrapment in polysiloxane-coated porous silica *J. Chromatogr.* **347** 11–23
- [4] Reetz M T, Tielmann P, Wiesenhofer W, Konen W and Zonta A 2003 Second generation sol–gel encapsulated lipases: robust heterogeneous biocatalysts *Adv. Synth. Catal.* **345** 717–28
- [5] Schmidtsteffen A and Staude E 1992 Ultrafiltration membranes for chemical binding of urease *Biotechnol. Bioeng.* **39** 725–31
- [6] Wei Y, Xu J, Feng Q, Dong H and Lin M 2000 Encapsulation of enzymes in mesoporous host materials via the non-surfactant-templated sol–gel process *Mater. Lett.* **44** 6–11
- [7] Lei C, Shin Y, Liu J and Ackerman E J 2002 Entrapping enzyme in a functionalized nanoporous support *J. Am. Chem. Soc.* **124** 11242–3
- [8] Lei C, Shin Y, Magnuson J K, Fryxell G, Lasure L L, Elliott D C, Liu J and Ackerman E J 2006 Characterization of functionalized nanoporous supports for protein confinement *Nanotechnology* **17** 5531–8
- [9] Deere J, Magner E, Wall J G and Hodnett B K 2002 Mechanistic and structural features of protein adsorption onto mesoporous silicates *J. Phys. Chem. B* **106** 7340–7
- [10] Han Y J, Stucky G D and Butler A 1999 Mesoporous silicate sequestration and release of proteins *J. Am. Chem. Soc.* **121** 9897–8
- [11] Han Y J, Watson J T, Stucky G D and Butler A 2002 Catalytic activity of mesoporous silicate-immobilized chloroperoxidases *J. Mol. Catal. B* **17** 1–8
- [12] Takahashi H, Li B, Sasaki T, Miyazaki C, Kajino T and Inagaki S 2000 Catalytic activity in organic solvents and stability of immobilized enzymes depend on the pore size and surface characteristics of mesoporous silica *Chem. Mater.* **12** 3301–5
- [13] Washmon L L and Balkus K J Jr 2000 Cytochrome c immobilized into mesoporous molecular sieves *J. Mol. Catal. B* **10** 453–69
- [14] Yiu H H P, Wright P A and Botting N P 2001 Enzyme immobilization using SBA-15 mesoporous molecular sieves with functionalised surfaces *J. Mol. Catal. B* **15** 81–92
- [15] Yiu H H P, Wright P A and Botting N P 2001 Enzyme immobilisation using siliceous mesoporous molecular sieves *Micropor. Mesopor. Mater.* **44/45** 763–8
- [16] Feng X, Fryxell G E, Wang L-Q, Kim A Y, Liu J and Kemner K M 1997 Functionalized monolayers on ordered mesoporous supports *Science* **276** 923–6
- [17] Zhao D Y, Feng J L, Huo Q S, Melosh N, Fredrickson G H, Chmelka B F and Stucky G D 1998 Triblock copolymer syntheses of mesoporous silica with periodic 50–300 angstrom pores *Science* **279** 548–52

- [18] Liu J, Shin Y, Nie Z M, Chang J H, Wang L-Q, Fryxell G E, Samuels W D and Exarhos G J 2000 Molecular assembly in ordered mesoporosity: a new class of highly functional nanoscale materials *J. Phys. Chem. A* **104** 8328–39
- [19] Baker N A, Sept D, Joseph S, Holst M J and McCammon J A 2001 Electrostatics of nanosystems: application to microtubules and the ribosome *Proc. Natl Acad. Sci. USA* **98** 10037–41
- [20] Honig B and Nicholls A 1995 Classical electrostatics in biology and chemistry *Science* **268** 1144–9
- [21] Honig B, Sharp K and Yang A S 1993 Macroscopic models of aqueous-solutions—biological and chemical applications *J. Phys. Chem.* **97** 1101–9
- [22] Sharp K A and Honig B 1990 Electrostatic interactions in macromolecules—theory and applications *Annu. Rev. Biophys. Biophys. Chem.* **19** 301–32
- [23] Dolinsky T J, Nielsen J E, McCammon J A and Baker N A 2004 PDB2PQR: an automated pipeline for the setup, execution, and analysis of Poisson–Boltzmann electrostatics calculations *Nucleic Acids Res.* **32** W665–7
- [24] Lei C, Shin Y, Liu J and Ackerman E J 2007 Synergetic effects of nanoporous support and urea on enzyme activity *Nano Lett.* **7** 1050–3
- [25] Minton A P 2001 The influence of macromolecular crowding and macromolecular confinement on biochemical reactions in physiological media *J. Biol. Chem.* **276** 10577–80
- [26] Minton A P 2006 Macromolecular crowding *Curr. Biol.* **16** R269–71
- [27] Zhou H-X and Dill K A 2001 Stabilization of proteins in confined spaces *Biochemistry* **40** 11289–93
- [28] Zhou H X 2004 Protein folding and binding in confined spaces and in crowded solutions *J. Mol. Recongnit.* **17** 368–75
- [29] Hecht H J, Kalisz H M, Hendle J, Schmid R D and Schomburg D 1993 Crystal structure of glucose oxidase from *Aspergillus niger* refined at 2.3 Å resolution *J. Mol. Biol.* **229** 153–72
- [30] Ye W-N and Combes D 1989 The relationship between the glucose oxidase subunit structure and its thermostability *Biochim. Biophys. Acta* **999** 86–93
- [31] Benning M M, Shim H, Raushel F M and Holden H M 2001 High resolution x-ray structures of different metal-substituted forms of phosphotriesterase from *Pseudomonas diminuta* *Biochemistry* **40** 2712–22